Electronic and optical properties of Au-doped Cu_2O: A first principles investigation

Jiang Zhong-Qian(姜中钱)[a)b)c)], Yao Gang(姚 钢)[b)c)], An Xin-You(安辛友)[b)], Fu Ya-Jun(符亚军)[b)], Cao Lin-Hong(曹林洪)[b)c)†], Wu Wei-Dong(吴卫东)[a)b)c)], and Wang Xue-Min(王雪敏)[b)‡]

[a)] *College of Science, Southwest University of Science and Technology, Mianyang* 621010, *China*

[b)] *Science and Technology on Plasma Physics Laboratory, Research Center of Laser Fusion, China Academy of Engineering Physics (CAEP), Mianyang* 621900, *China*

[c)] *Joint Laboratory for Extreme Conditions Matter Properties, Southwest University of Science and Technology and Research Center of Laser Fusion, China Academy of Engineering Physics (CAEP), Mianyang* 621010, *China*

(Received 19 September 2013; revised manuscript received 24 December 2013; published online 25 March 2014)

The Cu_2O and Au-doped Cu_2O films are prepared on MgO (001) substrates by pulsed laser deposition. The X-ray photoelectron spectroscopy proves that the films are of Au-doped Cu_2O. The optical absorption edge decreases by 1.6% after Au doping. The electronic and optical properties of pure and Au-doped cuprite Cu_2O films are investigated by the first principles. The calculated results indicate that Cu_2O is a direct band-gap semiconductor. The scissors operation of 1.64 eV has been carried out. After correcting, the band gaps for pure and Au doped Cu_2O are about 2.17 eV and 2.02 eV, respectively, decreasing by 6.9%. All of the optical spectra are closely related to the dielectric function. The optical spectrum red shift corresponding to the decreasing of the band gap, and the additional absorption, are observed in the visible region for Au doped Cu_2O film. The experimental results are generally in agreement with the calculated results. These results indicate that Au doping could become one of the more important factors influencing the photovoltaic activity of Cu_2O film.

Keywords: Cu_2O, electronic structure, optical properties, first-principles

PACS: 71.15.Ap, 71.20.−b, 71.22.+i, 78.66.−w **DOI:** 10.1088/1674-1056/23/5/057104

1. Introduction

Cuprous oxide (Cu_2O), as a p-type semiconductor with a direct band gap of 2.1 eV, possesses a set of unique optical and electronic properties. It is regarded as one of the most promising materials for photovoltaic application due to its low cost, nontoxicity, and high absorption rate in the visible region.[1] It has been extensively investigated for its applications in solar cell and optoelectronic devices.[2,3] The theoretical conversion efficiency is about 20%,[4] but the highest experimental efficiency is only about 2%.[5] This is due to the fact that the ionizing energy of the acceptor and free carrier concentration are low at ambient temperature, which is caused by the Cu vacancy and O interstitial atom.[1,6] Recently, a large number of studies reported that doping could improve the optical and electronic properties of Cu_2O. Ivill *et al.*[7] prepared the epitaxial films of Mn-doped Cu_2O by pulsed laser deposition (PLD). The ferro-electric properties of Cu_2O are enhanced, and a new peak (735 nm) has been observed in the photoluminescence spectrum at 700°C. The epitaxial films of Ni doped Cu_2O were grown also by PLD.[8] It was found that the vacancy mobility decreases in high concentration Ni doped Cu_2O film. The reason for this is that the vacancy carriers are scattered by the scattering center. Nakanko *et al.*[9] prepared the N-doped Cu_2O films using magnetron sputtering. N incorporation leads to the forbidden gap of Cu_2O broadening, which is consistent with the calculated results by Pu *et al.*[10] The electronic properties of Ag-, Ni-, and Zn-doped Cu_2O films were calculated by Martinez-Ruiz *et al.*[11] Ag 4d and O 2p orbits give rise to hybridization, and the band gap prominently decreases after Ag doped Cu_2O. Au doping can improve the transmissions of photoelectron and vacancy, and reduce recombinations of electron-hole pairs because of the formation of impurity level,[12,13] which can enhance the visible absorption, and reduce the absorption efficiency of ultraviolet (UV) light.[14,15]

Our team successfully fabricated the single oriented Cu_2O (011) films on MgO (001) substrates at temperatures ranging from 450 °C to 600 °C by PLD. The optical band gap of Cu_2O film was determined by the linear extrapolation method.[16] Hence, in order to further study the optical properties of Cu_2O film, we firstly study the optical properties of Au-doped Cu_2O film with theoretical methods, using the first principles calculation that is one of the most powerful tools for the theoretical investigation of solid properties.[17] In this work, the electronic and optical properties of pure and Au-doped cuprite Cu_2O films are investigated by the first principles. Meanwhile, the Cu_2O and Au-doped Cu_2O films are prepared by PLD, and part of the computational results are

†Corresponding author. E-mail: hyclh@yeah.net

‡Corresponding author. E-mail: wangxuemin75@sohu.com

© 2014 Chinese Physical Society and IOP Publishing Ltd

compared with the experimental results.

2. Experimental and computational methods

2.1. Calculation

At ambient temperature and pressure, the stable phase of Cu_2O is a cubic cuprite structure with a $Pn\bar{3}M$ ($224^{\#}$) space group. Its lattice constants are $a = b = c = 0.427$ nm, $\alpha = \beta = \gamma = 90°$.[18] The lattice cells of copper and oxygen form the cubic structure from the accumulation of reverse. All the calculations are based on the supercell model as shown in Fig. 1(a). The $2 \times 2 \times 1$ Cu_2O supercell, which contains 16 Cu atoms and 8 O atoms is considered. Cu atoms are directly replaced at high symmetric points (1/8, 3/8, 3/4) with Au atoms. The concentration is 6.25%. This supercell contains only one Au atom in order to avoid interaction between doping atoms. In the system of Au doped Cu_2O, the symmetry of the supercell is destroyed. According to the symmetry of Au doped Cu_2O, the different atoms are classified into Cu: 1, 7, 9 (I); 4 (II); 6, 8 (III); 2, 3, 5 (IV); O: 1, 2, 3, 5 (I); 4, 6 (II), and the model of Au-doped supercell structure is shown in Fig. 1(b).

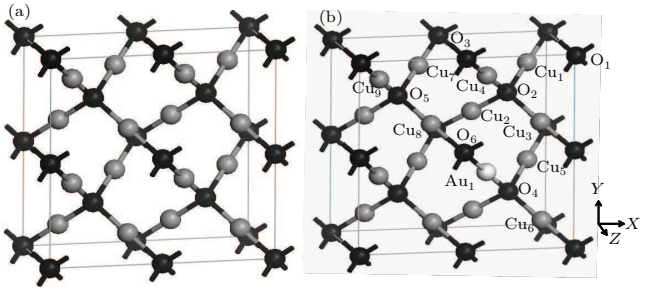


Fig. 1. Structures of pure (a) and Au-doped (b) Cu_2O.

The calculations were performed with the Cambridge Serial Total Energy Package (CASTEP) code,[19,20] which is based on the density function theory using a plane-wave pseudopotential method. The exchange–correlation function is described by the generalized gradient approximation (GGA) in the scheme of Perdew–Burke–Ernzerhof (PBE).[21,22] The ultrasoft pseudopotential[23] was used with $3d^{10}4s^1$, $2s^22p^4$, and $5d^{10}6s^1$ as the valence-electron configuration for the copper, oxygen and gold atoms, respectively. The electron wave function was expanded in the plane-wave basis set with a cutoff energy of 450 eV, and a Monkhorst–Pack grid[24] with parameters of $3 \times 3 \times 6$ $\boldsymbol{k}$-point was used for an irreducible Brillouin zone sampling. To ensure the proper convergence of the self-consistency calculation, the total energy was converged to less than 5.0×10^{-6} eV/atom. The crystal structures and the atom coordinates were fully relaxed without any restriction by using the Broyden Fletcher Goldfarb Shanno method[25] until the forces on each atom converged to less than 0.01 eV/Å, the stress below 0.02 GPa and the displacement of atoms during the geometry optimization was less than 5×10^{-4} Å.

2.2. Experiment

The Cu_2O and Au-doped Cu_2O films were prepared on MgO (001) substrates by PLD. A sintered CuO target (50 mm in diameter) with a purity of 99.9% was prepared. A chip of 99.99% pure Au was uniformly placed onto the surface of the CuO target. The area ratio of the Au piece to the CuO target was 1/8. The target was mounted on a rotating holder, 50 mm away from the MgO (001) substrates. In the PLD processing, a KrF-excimer laser beam measuring 248 nm in wavelength and 20 ns in pulse duration was used as the laser source. Before the deposition, the PLD chamber was vacuumed to a based pressure of $\sim 2 \times 10^{-7}$ Pa. The films were prepared under the conditions which were described in detail elsewhere.[16] *In situ* X-ray photoelectron spectroscopy (XPS) with Mg Kα (1253.6 eV) exciting radiation was used to analyze the chemical composition and the Au concentration in each of the films. The linear optical absorption spectra of the films was detected by a double beam (UV)-VIS spectrophotometer.

3. Results and discussion

3.1. XPS results

The XPS results of Cu 2p and Au 4f photoelectron core levels are shown in Fig. 2. As indicated in Fig. 2(d), the peaks of Au $4f_{7/2}$ and Au $4f_{5/2}$ are located at positions of 84.00 eV and 87.65 eV, respectively, and as shown in Figs. 2(a)–2(c), the Cu 2p core-level results are in good agreement with those in Ref. [16], which indicates that the Cu in oxidation state is Cu^+. These results prove that these films are all Au-doped Cu_2O films. The concentration [Au/(Au+ Cu), at.%] of the sample can be derived from the XPS, which is about 8.18 at.%.

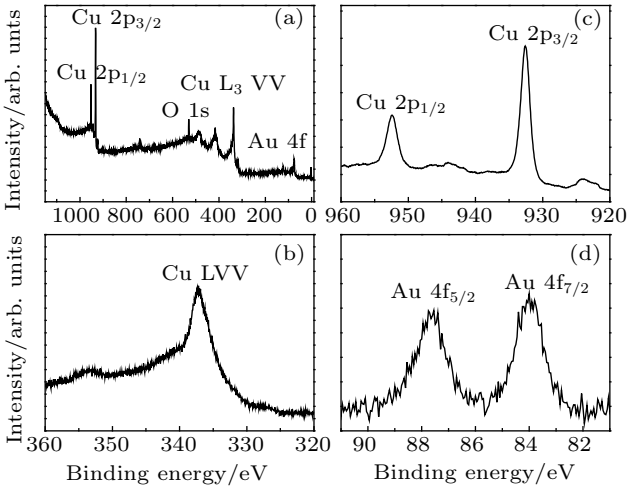


Fig. 2. X-ray photoelectron spectra of the Au:Cu_2O films, showing (a) overview XPS spectrum of the products, and spectra of (b) Cu LVV, (c) Cu 2p, (d) Au 4f.

3.2. Structural parameters

At a temperature and pressure of zero, equilibrium lattice constants of pure and Au-doped Cu_2O are $a = b = c = 4.30$, 4.35 Å, respectively. The results are in reasonable agreement

with other experimental and calculated data.[13,18,26–31] The primitive cell volumes of pure and Au-doped Cu_2O are both 79.75, 81.81 Å^3. The lattice constants and primitive cell volumes of Au-doped Cu_2O increase because the radius of Au^+ (0.137 nm) is larger than that of Cu^+ (0.096 nm). The total energies of before and after Au doping are −25035.24 eV and −24601.58 eV, respectively. The detailed results are listed in Table 1.

Table 1. Values of lattice constant (a), volume (V), and band gap (E_g) of pure and Au-doped Cu_2O.

	Cu_2O	Au-doped	Other results
a/Å	4.30	4.35	4.27,[18] 4.267,[26] 4.31,[27] 4.30,[13] 4.314,[28] 4.32,[29] 4.34,[30] 4.28[31]
V/Å^3	79.75	81.81	77.77,[18] 80.06,[27] 79.51[12]
E_g/eV	0.53	0.38	2.17,[18] 2.10,[32] 2.52,[33] 0.70[27] 0.50,[13] 0.46,[34] 0.43,[35] 0.47[36]

3.3. Electronic properties

In order to analyze the optical properties of pure and Au-doped Cu_2O, we first investigate their electronic properties based on the optimization. The band structure of pure Cu_2O is shown in Fig. 3(a). The Fermi level is located at 0 eV. The pure Cu_2O is a direct band-gap semiconductor. The band gap is about 0.53 eV at high symmetric Γ point, which is obviously less than the experimental value of 2.17 eV.[18] It is well known that the underestimated band gap can be attributed to the choice of exchange–correlation energy.[37] This issue is very critical when considering donors, but it has a relatively weak influence on energies of acceptor levels which are derived from the valence states. For pure Cu_2O, since the energies of calculated Cu 3d states are overestimated, the interaction between Cu 3d and O 2p states increases and the band gap decreases, which can cause the top of the valence band to shift toward the high energy region. The calculated results can be corrected with a scissors operation.[38–40] The band structure of pure Cu_2O under a 1.64 eV scissors operation is shown in Fig. 3(b), and the band gap is 2.17 eV. The band structure of Au doped Cu_2O is presented in Fig. 4(a), the band gap (0.38 eV) decreases by 28.3%. After correcting, as shown in Fig. 4(b), the band gap is 2.02 eV, the change value is 0.15 eV, decreasing by 6.9%. Under the action of vicinity O atoms, the degeneracy of energy level drops off and Au 5d states split when the Cu atom is replaced by an Au atom. In addition, Au is a transition metal, the spin exchange between local spin states and the sp band result in the valence and conduction bands shifting towards a low energy region, and the shift of valence band is larger than conduction band.

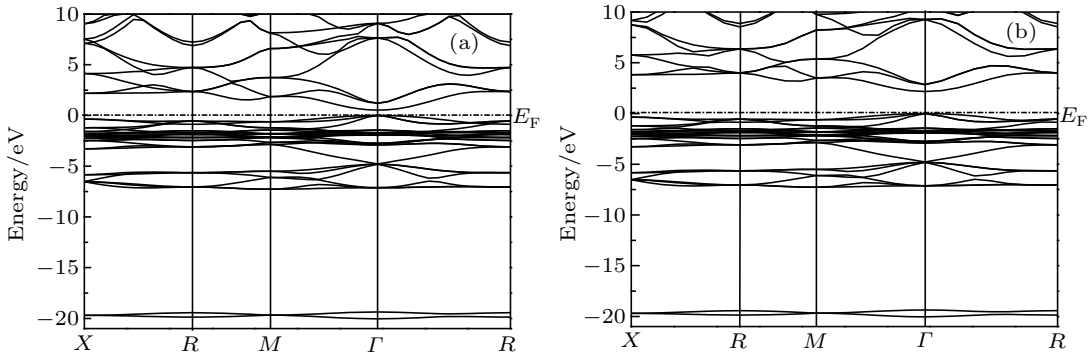


Fig. 3. Band structures of pure Cu_2O: (a) before correcting, (b) after correcting. The symmetry points of first Brillouin zone: $\Gamma(0, 0, 0)$, $M(1/2, 1/2, 0)$, $R(1/2, 1/2, 1/2)$, and $X(1/2, 0, 0)$.

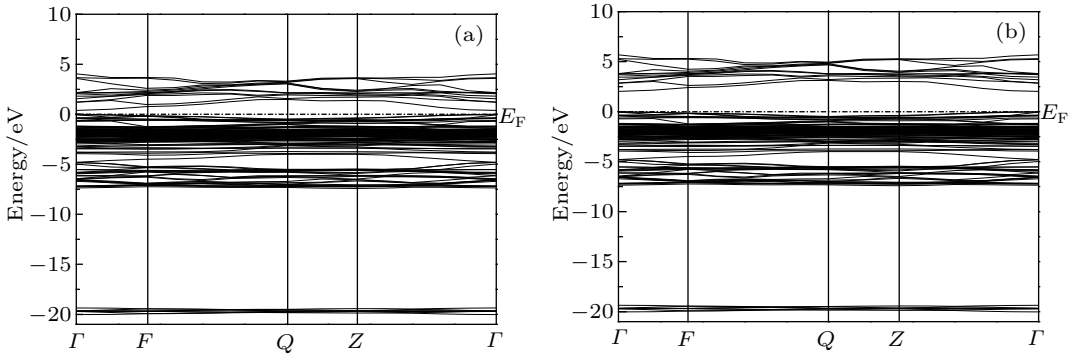


Fig. 4. Band structures of Au:Cu_2O: (a) before correcting, (b) after correcting. The symmetry points of first Brillouin zone: $\Gamma(0, 0, 0)$, $F(0, 1/2, 0)$, $Q(0, 1/2, 1/2)$, and $Z(0, 0, 1/2)$.

The total and partial densities of states of pure Cu_2O are presented in Fig. 5(a). The conduction band mainly derives from the Cu 4s states, and the valence band mainly consists of the Cu 3d, O 2s, and 2p states. The O 2s states are predominantly found between −20.3 eV and −18.9 eV while the O 2p states appear in a range of −7.3 eV to −5.9 eV. The calculated O 2s and 2p states described in the present work are in reasonable agreement with experimental results.[41,42] In the uppermost valence band, Cu 3d states are obviously observed between −4.5 eV and 0 eV. The total and partial densities of states of Au-doped Cu_2O are shown in Fig. 6(a). There is a distribution between −4.8 eV and 0 eV which mainly derives from the Au 5d states. Both Au 5d and Cu 3d states form the hybrid orbital with O 2p states, which leads to the redistribution of the energy of Au-doped Cu_2O system. Conduction bands shift to the Fermi level. The forbidden bandwidth narrows down. These results are consistent with the above results of band structures. Finally, the total and partial densities of states of pure and Au-doped Cu_2O under a 1.64 eV scissors operation are shown in Figs. 5(b) and 6(b).

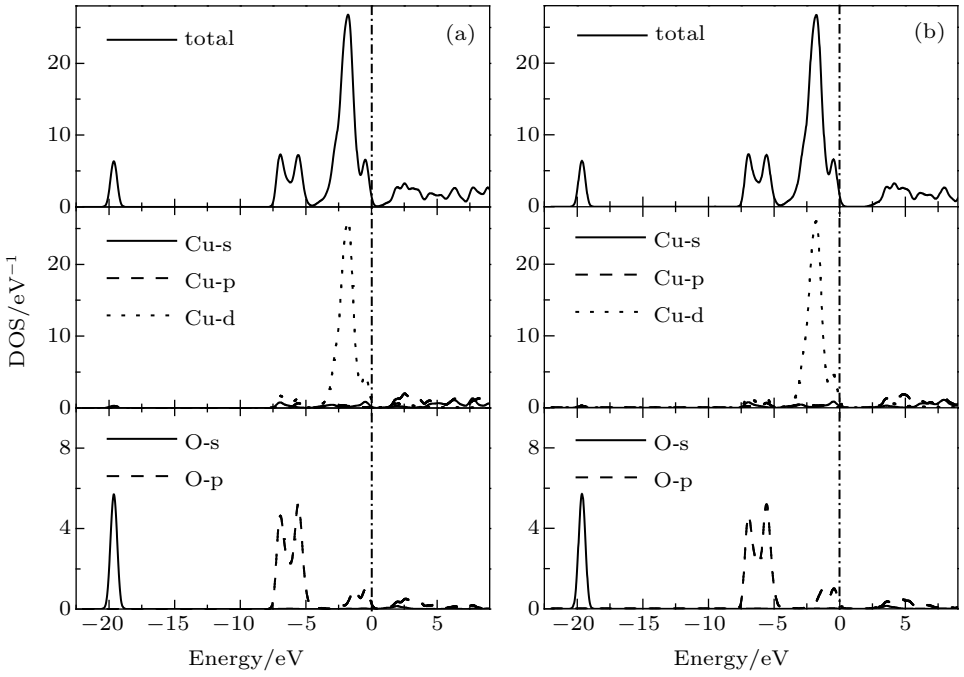


Fig. 5. Total and partial densities of states of pure Cu_2O: (a) before correcting, (b) after correcting.

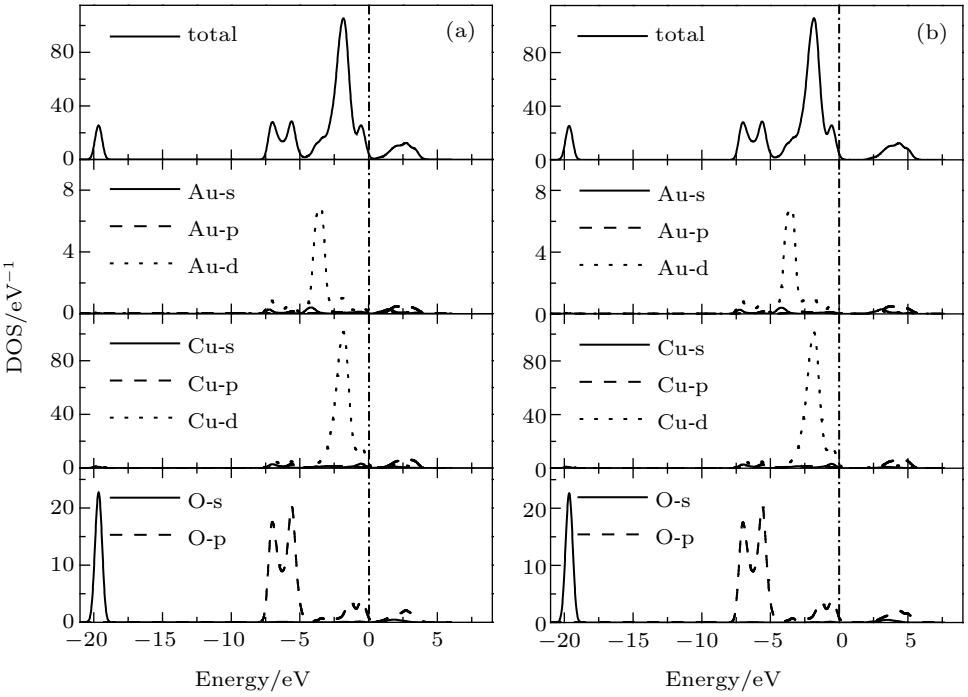


Fig. 6. Total and partial densities of states of Au:Cu_2O: (a) before correcting, (b) after correcting.

The Mulliken population analysis[43,44] is a good method to study bonding behavior and to understand the charge transfer between the cation and anion. The calculated population analyses of pure and Au-doped Cu_2O are listed in Table 2. The positive value of the charge represents the lost electron, and the negative refers to the accepted electron. For the pure Cu_2O, the Mulliken charge distribution mainly consists of O 2p and Cu 3d states. Accepting and losing electrons is related to the variety of elements and the electronegativity of vicinal atoms. For Au-doped Cu_2O, the Mulliken charge distribution mainly derives from the O 2p, Cu 3d, and Au 5d states. The charges of O (II) near the Au atom decrease from $-0.67e$ to $-0.65e$ (the negative sign represents accepting an electron), but the charges of Cu (II) and Cu (IV) increase. The average charge of Cu (I $\sim$ IV) ($0.34e$) is more than Au ($0.20e$). It is indicated that the Cu atom has a strong ability to lose an electron compared with an Au atom, and the interactions of Au with the vicinal atoms are weaker in the Au-doped Cu_2O system. We also investigate the Mulliken overlap populations[43,45] of pure and Au doped Cu_2O to describe the interaction between atoms as listed in Table 3. The positive overlap populations indicate the bonding between atoms, while the negative represents anti-bonding, and the value refers to the intensity of bonding. It is found that pure and Au-doped Cu_2O are both covalent chemical bonding materials. The Mulliken overlap population of O (II)–Au is about 0.25, and a weak covalent chemical bonding exists in O (II)–Au. The population of O–Cu (III) increases from 0.33 to 0.39 after Au doping. It indicates that the outer shell electrons of Au atoms play a significant role in the vicinal atoms after Au atoms have been doped in Cu_2O. In addition, the bond lengths of Au–O are larger than Cu–O, which is one of the main reasons for the volume increase of Au-doped Cu_2O.

Table 2. Mulliken charge distributions of pure and Au-doped Cu_2O.

Species		Ion	s	p	d	Total	Charge/e
Pure	Cu	1–9	0.58	0.45	9.64	10.67	0.33
	O	1–6	1.82	4.85	—	6.67	−0.67
Au-doped	Cu	1, 7, 9 (I)	0.58	0.45	9.64	10.67	0.33
		4 (II)	0.58	0.44	9.64	10.66	0.34
		6,8 (III)	0.58	0.44	9.63	10.66	0.34
		2, 3, 5 (IV)	0.59	0.43	9.63	10.65	0.35
	O	1, 2, 3, 5 (I)	1.82	4.85	—	6.67	−0.67
		4, 6 (II)	1.83	4.81	—	6.65	−0.65
	Au	1	0.81	0.41	9.59	10.80	0.20

Table 3. Mulliken overlap populations of overlap populations for pure and Au-doped Cu_2O.

	Bond	Population	Length/Å
Pure	O–Cu	0.33	1.86387
Au-doped	O (I)–Cu (I)	0.36	1.86677
	O (I)–Cu (II)	0.38	1.86773
	O (I)–Cu (III)	0.37	1.86332
	O (I)–Cu (IV)	0.37	1.86363
	O (II)–Cu (III)	0.39	1.86352
	O (II)–Cu (IV)	0.38	1.85860
	O (II)–Au	0.25	2.14719

3.4. Optical properties

The complex dielectric function $\varepsilon(\omega) = \varepsilon_1(\omega) + \mathrm{i}\varepsilon_2(\omega)$ is known to describe the optical properties of materials. In this work, the excitonic effect is ignored while the local field effect is included in the calculation. The imaginary part $\varepsilon_2(\omega)$ is calculated from the momentum matrix elements between the occupied and unoccupied wave functions within the selection rules. Transitions between occupied and unoccupied states are caused by photon absorption or emission. The real part $\varepsilon_1(\omega)$ of the complex dielectric function can be obtained using the Kramers–Kronig relationship. The imaginary part $\varepsilon_2(\omega)$ and the real part $\varepsilon_1(\omega)$ of the dielectric function $\varepsilon(\omega)$ are given respectively, by[46–50]

$$\varepsilon_2(\omega) = \left(\frac{4\pi^2 e^2}{m^2\omega^2}\right)\sum_{i,j}\int_k \langle i|M|j\rangle^2 f_i(1-f_i) \times \delta\left(E_{j,k} - E_{i,k} - \omega\right) \mathrm{d}^3k, \quad (1)$$

$$\varepsilon_1(\omega) = 1 + \frac{2}{\pi}P\int_0^\infty \frac{\omega'\varepsilon_2(\omega')\,\mathrm{d}\omega'}{(\omega'^2 - \omega^2)}, \quad (2)$$

where e is the charge of a free electron, m is the mass of a free electron, ω is the frequency of incident photon, M is the dipole matrix, i and j are the initial and final states respectively, f_i is the Fermi distribution function for the i-th state, E_i is the energy of electron in the i-th state with crystal wave vector k, and P denotes the principal value of the integral. Optical constants such as absorption coefficient $I(\omega)$, refractive index $n(\omega)$, extinction coefficient $k(\omega)$ electron energy loss spectrum $L(\omega)$ and optical reflectivity $R(\omega)$ can be obtained. The concerned formulas are as follows:

$$I(\omega) = \sqrt{2}(\omega)\left[\sqrt{\varepsilon_1(\omega)^2 + \varepsilon_2(\omega)^2} - \varepsilon_1(\omega)\right]^{1/2}, \quad (3)$$

$$n(\omega) = \left[\frac{\sqrt{\varepsilon_1(\omega)^2 + \varepsilon_2(\omega)^2}}{2} + \frac{\varepsilon_1(\omega)}{2}\right]^{1/2}, \quad (4)$$

$$k(\omega) = \left[\frac{\sqrt{\varepsilon_1(\omega)^2 + \varepsilon_2(\omega)^2}}{2} - \frac{\varepsilon_1(\omega)}{2}\right]^{1/2}, \quad (5)$$

$$L(\omega) = \frac{\varepsilon_2(\omega)}{\varepsilon_1(\omega)^2 + \varepsilon_2(\omega)^2}, \quad (6)$$

$$R(\omega) = \left|\frac{\sqrt{\varepsilon(\omega)} - 1}{\sqrt{\varepsilon(\omega)} + 1}\right|^2. \quad (7)$$

The real and imaginary parts of the dielectric function for pure and Au-doped Cu_2O are displayed in Fig. 7 From the real part of dielectric function $\varepsilon_1(\omega)$, the information about the electronic polarizability of the material can be obtained. The static dielectric constants at the zero frequency limit of pure and Au-doped Cu_2O are 9.34 and 8.92, respectively. Two negative distributions are observed in the ranges of 3.97 eV–5.79 eV and 11.65 eV–18.86 eV for pure Cu_2O, but only one negative distribution is observed between 3.56 eV and 11.64 eV for Au-doped Cu_2O. It indicates that pure and Au-doped Cu_2O each show a metallic behavior in these frequency

zones. In the curve $\varepsilon_2(\omega)$, there are mainly three peaks identified by symbols A (11.96 at 3.25 eV), B (3.25 at 7.55 eV), C (4.88 at 11.79 eV) for pure Cu_2O. The peak A mainly derives from the transition from Cu 3d states (the top of valence band) to the O 2p states (the bottom of conduction band) at Γ-point. The peaks B and C mainly contribute to the transition from Cu 4s to O 2p states. There are only two peaks which are identified by the symbols A' (11.96 at 3.39 eV) and B' (1.78 at 7.62 eV) for Au-doped Cu_2O. The intensities of peaks A and A' are almost the same, but peak B' is weaker than peak B. The peak C' (unlabelled) vanishes at 11.79 eV. This is due to the split of energy levels after Au has been doped in Cu_2O. The valence bands shift to the Fermi level, and the transitions are forbidden at higher energy bands.

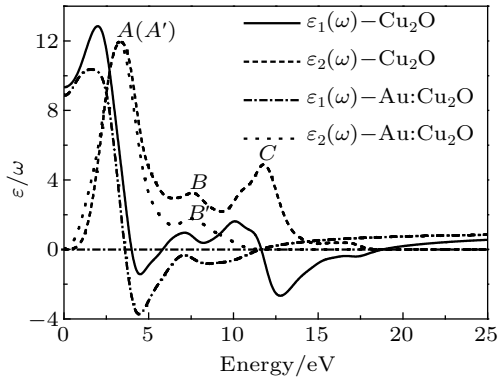


Fig. 7. Real $\varepsilon_1(\omega)$ and imaginary $\varepsilon_2(\omega)$ parts of the dielectric function for pure and Au-doped Cu_2O.

The absorption edge E_g can be described by the following relation:[51]

$$\alpha h\nu = C\left(h\nu - E_g\right)^n, \tag{8}$$

where $h\nu$ is the photon energy, C is a constant, and α is the optical absorption coefficient. The value $n = 1/2$ is used for a direct band gap material and $n = 2$ for an indirect band gap material.

For a semiconductor, the change of the band gap has a great influence on optical properties. In this work, the optical absorption edges are calculated from Eq. (8), and the calculated results are shown in Fig. 8(b). With the linear extrapolation method, the direct absorption edges for pure and Au-doped Cu_2O are obtained to be 3.04 eV and 2.99 eV, respectively. In order to verify the reliability of the calculated results, the optical band gaps of pure and Au-doped Cu_2O are analyzed from the experimental results. The experimental results are shown in Fig. 9(b). The optical absorption edges for pure and Au-doped Cu_2O are found to be 2.47 eV and 2.43 eV respectively. The experimental results for pure Cu_2O are consistent with Fu *et al.*'s result of (2.46 eV).[16] The calculated and measured optical absorption edges each decrease by 1.6% after Au doping, which indicates that the measured results are generally in agreement with the calculated results.

As shown in Fig. 8(a), the absorption spectra shifts to the low energy region, which is due to the interband transition of excitation electrons. The enhancement of absorption can be observed in the visible region (1.5 eV $\sim$ 3.5 eV) as shown in the inset of Fig. 8(a) for Au-doped Cu_2O, which is due to the interband transition between Au 5d and O 2p states. The absorption region is quite wide (1.23 eV $\sim$ 18.81 eV for pure Cu_2O and 0.57 eV $\sim$ 11.69 eV for Au-doped Cu_2O), but the main absorption part is still located in the UV region. The absorption of Au doped disappears when the photon energy is more than 13.03 eV. As a result, the absorption obviously decreases in the UV region and increases in the visible region after the Au doping. The experimental absorptions are shown in Fig. 9(a). The absorption coefficient increases in a range of 1.5 eV $\sim$ 3.0 eV after doping, which indicates that the theoretical and the experimental values are consistent with each other in the visible region. The inset of Fig. 9(b) shows that the transmissivity is enhanced in the UV region (3.5 eV $\sim$ 6.0 eV), but reduced in the visible region (1.5 eV $\sim$ 3.0 eV), which may be induced by the enhancement of absorption. These results indicate that Au doping could become one of the most important factors influencing the photovoltaic activity of Cu_2O.

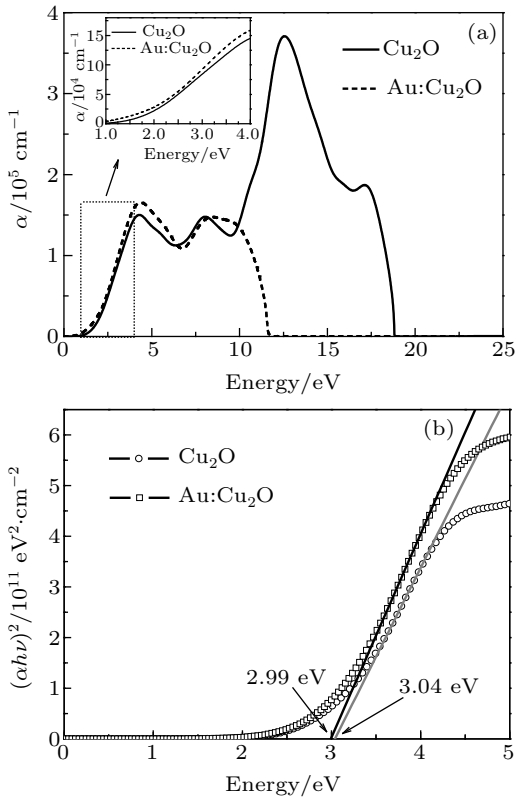


Fig. 8. Calculated absorption coefficients $I(\omega)$ (a) and optical absorption edges (b) of pure and Au-doped Cu_2O.

The calculated values of refractive index$n(\omega)$ and the extinction coefficient $k(\omega)$ of pure and Au-doped Cu_2O are displayed in Figs. 10(a) and 10(b) respectively. The values of static refractive index $n(0)$ are 3.06 (pure) and 2.99 (Au-doped). The maximum refractive indices are 3.67 eV at 2.19 eV (pure) and 3.32 at 2.06 eV (Au doped). The refractive indices decrease to their minimum levels in the UV region. In the curves of $k(\omega)$, the local maxima of the extinction coefficient $k(\omega)$ correspond to the zero of $\varepsilon_1(\omega)$ ($\approx$ 3.99 eV and

3.96 eV, respectively). The origin of the structure in the imaginary part of the dielectric function also explains the structure in the refractive index.[25]

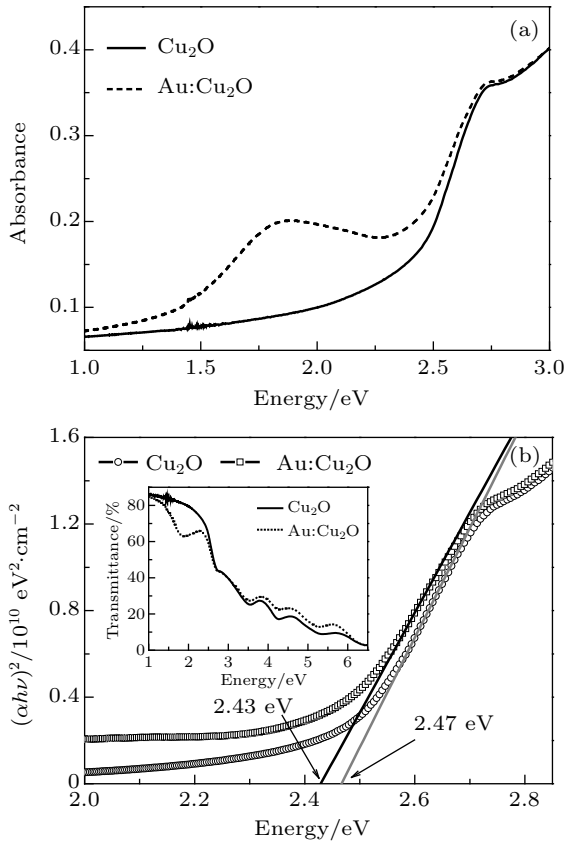


Fig. 9. Measured absorbance (a) and optical absorption edges (b) of pure and Au-doped Cu_2O. The inset shows the corresponding optical transmission spectrum.

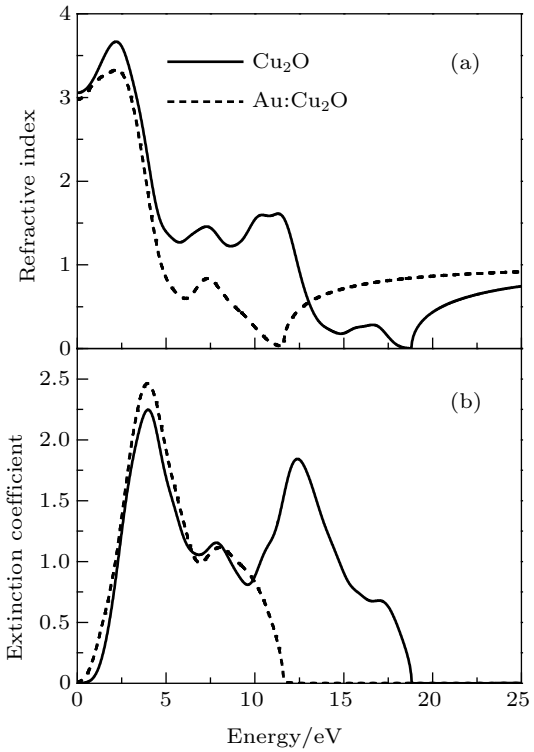


Fig. 10. Curves of refractive index $n(\omega)$ (a) and extinction $k(\omega)$ (b) versus energy of pure and Au-doped Cu_2O.

The loss function is an important parameter to describe the energy loss of a fast electron traversing in a material. Generally, the peak of the $L(\omega)$ spectrum represents the characteristic associated with the plasma resonance and the corresponding frequency is the so-called plasma frequency ω_p.[51] Figure 11(a) shows that the resonant energy losses of pure and Au-doped Cu_2O occur at 18.82 eV and 11.60 eV, respectively. The values of the reflectivity $R(\omega)$ of pure and Au-doped Cu_2O are displayed in Fig. 11(b). The values of zero-frequency reflectivity are 25.7% (pure) and 24.8% (Au-doped), and the maximum values of reflectivity are observed at 18.79 eV and 11.55 eV, respectively. Since the absorption is weak ($\alpha \approx 0$ cm^{-1}) and the reflectivity quickly drops off in the high energy region ($>$ 18.79 eV for pure Cu_2O and $>$ 11.55 eV for Au-doped Cu_2O), the values of transmissivity are obviously enhanced in the UV region. Remarkably, once the maximum of energy loss function occurs, the reflectivity starts to decrease most rapidly as shown in Figs. 11(a) and 11(b).

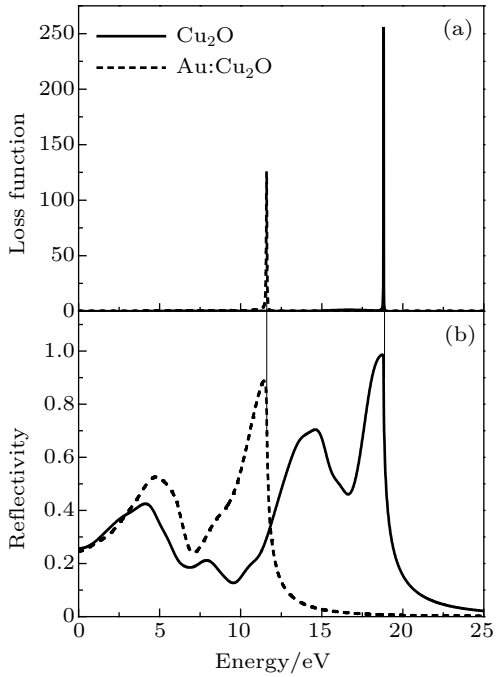


Fig. 11. Curves of loss function $L(\omega)$ (a) and reflectivity $R(\omega)$ (b) versus energy of pure and Au-doped Cu_2O.

4. Conclusions

In this paper, the Cu_2O and Au-doped Cu_2O films are successfully prepared on MgO (001) substrates by pulsed laser deposition. The electronic and optical properties of pure and Au-doped cuprite Cu_2O are investigated. The optimized lattice constant is in good agreement with other experimental and calculated data. The calculated results indicate that Cu_2O is a direct band-gap semiconductor. The band gap corrected by a scissors operation decreases by 6.9% after Au doping, and the experimental result is 1.6%. The interband contribution to the optical response function with the band structure is analyzed.

The O 2p, Cu 3d, and Au 5d states play a major role in the optical properties of pure and Au-doped Cu_2O. All of the optical spectra are closely related to the dielectric function. The optical spectrum red shift is corresponding to the decrease of the band gap. The enhancements of the calculated and the measured absorption both can be observed in the visible region after Au doping. These results provide a basis for further research on the optical properties of Cu_2O.

References

[1] Rakhshani A E 1986 *Solid State Electronics* **29** 7
[2] Ghisjen J, Tjeng L H, Elp J, Eskes H, Westerink J, Sawatzky G A and Czyzyk M T 1988 *Phys. Rev. B* **38** 11322
[3] Matsuzaki K, Ishizuka S, Yanagita M, Nawa Y, Goutam K P and Sakurai T 2006 *Solar Energy* **80** 715
[4] Olsen L C, Addis F W and Miller W 1982 *Solar Cells* **7** 247
[5] Mittiga A, Salza E and Sarto F 2006 *Appl. Phys. Lett.* **88** 163502
[6] Mizuno K, Izaki M, Murase K, Shinagawa T, Chigane M, Inaba M, Tasaka A and Awakura Y 2005 *J. Electr. Chem. Soc.* **152** C179
[7] Ivill M, Overberg M E, Abernathy C R and Norton D P 2003 *Solid-State Electronics* **47** 2215
[8] Kikuchi N and Tonooka K 2005 *Thin Solid Films* **486** 33
[9] Nakano Y, Saeki S and Morikawa T 2009 *Appl. Phys. Lett.* **94** 022111
[10] Pu C Y, Li H J and Tang X 2012 *Acta Phys. Sin.* **61** 047104 (in Chinese)
[11] Martinez-Ruiz A, Moreno M G and Takeuchi N 2003 *Solid State Science* **5** 291
[12] Bamwenda G R, Tsubota S, Nakamura T and Haruta M J 1995 *J. Photochem. Photobio. A: Chem.* **89** 177
[13] Khan M M and Cho M H 2012 *Bull. Korean Chem. Soc.* **33** 1753
[14] Subramanian V, Wolf E E and Kamat P V 2003 *Langmuir* **19** 469
[15] Zang L, Macyk W, Lang C, Maier W F, Antonius C, Meissner D and Kisch H 2000 *Chem. Eu. J.* **6** 379
[16] Fu Y J, Lei H W, Wang X M, Yan D W, Cao L H, Yao G, Shen C L, Peng L P, Zhao Y, Wang Y Y and Wu W D 2013 *Appl. Sur. Sci.* **273** 19
[17] Okoye C M I 2003 *J. Phys: Condens. Matter* **15** 5945
[18] Kirfel A and Eichhorn K D 1990 *Acta Crystal. A* **46** 271
[19] Segall M D, Lindan P J D, Probert M J, Pickard C J, Hasnip P J, Clark S J and Payne M C 2002 *J. Phys.: Condens. Matter* **14** 2717
[20] Liu L, Wei J J, An X Y, Wang X M, Liu H N and Wu W D 2011 *Chin. Phys. B* **20** 106201
[21] Ren D H and Cheng X L 2012 *Chin. Phys. B* **21** 127103
[22] Perdew J P and Zunger A 1981 *Phys. Rev. B* **23** 5048
[23] Vanderbilt D 1990 *Phys. Rev. B* **41** 7892
[24] Monkhorst H J and Pack J D 1976 *Phys. Rev. B* **13** 5188
[25] Bouhemadou A, Djabi F and Khenata R 2008 *Phys. Lett. A* **372** 4527
[26] Restori R and Schwarzenbach D 1986 *Acta Crystallogr.* **42** 201
[27] Mazharul M I, Boubakar D, Vincent M and Philippe M 2009 *J. Mol. Struc.: THEOCHEM* **903** 41
[28] Li C, Wang F, Li S F and Jia Y 2010 *Phys. Lett. A* **374** 2994
[29] Soon A, Todorova M, Delley B and Stampfl C 2007 *Phys. Rev. B* **75** 125420
[30] Soon A, Söhnel T and Idriss H 2005 *Surf. Sci.* **579** 131
[31] Ruiz E, Alvarez S, Alemang P and Evarestov R A 1997 *Phys. Rev. B* **56** 7189
[32] Masaya I and Song Y 2011 *Jpn J. Appl. Phys.* **50** 051002
[33] Wong L M, Chiam S Y, Huang J Q, Wang S J, Pan J S and Chim W K 2010 *J. Appl. Phys.* **108** 033702
[34] Soon A, Cui X Y, Delley B, Wei S H and Stampfl C 2009 *Phys. Rev. B* **79** 035205
[35] Raebiger H, Lany S and Zunger A 2007 *Phys. Rev. B* **76** 045209
[36] Nolan M and Elliott S D 2006 *Phys. Chem. Chem. Phys.* **8** 5350
[37] Zhang X D, Guo M L, Liu C L, Li W X and Hong X F 2008 *Appl. Phys. Lett.* **93** 012103
[38] Lin Z, Orlov A, Lambert R M and Payne M C 2005 *J. Phys. Chem. B* **109** 20948
[39] Yang K, Dai Y and Huang B 2007 *J. Phys. Chem. C* **111** 12086
[40] Zhang X D, Guo M L, Li W X and Liu C L 2008 *J. Appl. Phys.* **103** 063721
[41] Ghisjen J, Tjeng L H, Elp J, Eskes H, Westerink J, Sawatsky G A and Czyzyk M T 1988 *Phys. Rev. B* **38** 11322
[42] Ghijsen J, Tjeng L H, Eskes H, Sawatsky G A and Johnson R L 1990 *Phys. Rev. B* **42** 2268
[43] Mulliken R S 1955 *J. Chem. Phys.* **23** 1833
[44] Segall M D, Pickard C J, Shah R and Payne M C 1996 *Mol. Phys.* **89** 571
[45] Segall M D, Shah R, Pickard C J and Payne M C 1996 *Phys. Rev. B* **54** 16317
[46] Ambrosch D C and Sofo J O 2006 *Comput. Phys. Commun.* **175** 1
[47] Yao G, Chen Y, An X Y, Jiang Z Q, Cao L H, Wu W D and Zhao Y 2013 *Chin. Phys. Lett.* **30** 067101
[48] Fox M 2001 *Optical Properties of Solids* (New York: Oxford University Press)
[49] Yang Z J, Guo Y D, Li J, Liu J C, Dai W, Cheng X L and Yang X D 2010 *Chin. Phys. B* **19** 077102
[50] Srikant V and Clarke D R 1997 *J. Appl. Phys.* **81** 6357
[51] Anderson O L 1963 *J. Phys. Chem. Solids* **24** 909